# IDENTIFICATION OF BEARING AND SEAL DYNAMIC STIFFNESS PARAMETERS BY STEADY STATE LOAD AND SQUEEZE FILM TESTS

Donald E. Bently and Agnes Muszynska
Bently Rotor Dynamics Research Corporation
Minden, Nevada 89423

This paper presents the results of two simple tests, mainly steady state load test and squeeze film test, for establishing the coefficients of bearings and seals. It also discusses methodology of the tests and some observed conclusions from the obtained data. In the last chapter, perturbation testing results are given as an example of verification and proof of validity of the two previous tests.

## INTRODUCTION

In several previous papers [1-5], the utilization of perturbation methodology to identify the dynamic stiffness characteristics of cylindrical seals and bearings has been shown. These studies were deliberately limited to low eccentricity, with the rotor statically centered and with maximum motion limited to 0.6 eccentricity ratio, and produced very satisfactory results.

However, in our first attempts to observe the rotor/bearing stiffness characteristics by perturbation testing at high static eccentricities, as reported in [4], great difficulties were encountered because of the effects of the cross coupled nonlinearities of the various dynamic stiffness terms that we were attempting to evaluate. It was, therefore, necessary to retrench and develop more suitable techniques for evaluating dynamic stiffness terms at eccentricity ratios above 1/2. The first attempt was to run Squeeze Film Test (with rotative speed $\omega_R$ at zero), applying both a steady state load (to yield families of measurements from 0 to 0.8 eccentricity ratio) and then apply the circular perturbation force at various levels and speeds. Once more, a lot of effort was expended, but the results were once again not clear, as the nonlinearities of the dynamic stiffness terms were so intermeshed that they became very difficult to evaluate. The only good to come of this effort, besides showing how difficult these terms can be, was to show a different form of fluid inertia effect at very high eccentricities in squeeze film tests, which could be the results of what Dr. Hendricks of NASA Lewis calls "fluid film fracture fraction," which is an effect occurring when two flat surfaces in close proximity are separated. Since the latter did not appear to be vital to the stability situation of bearings and seals, this interesting phenomenon was not pursued.

Having learned a lot about what not to do, two elementary studies were then initiated. These tests are (i) the Steady State Loading Test (that has been successfully used in many studies across more than 80 years), and (ii) an equally simple Squeeze Film Test at Zero Eccentricity. These very limited, very simple studies yielded the desired results and proved quite successful in evaluation of the various dynamic stiffness terms. These two tests are shown herein, with several results and conclusions. Finally perturbation tests using from very low to very high input forces are shown to confirm the validity of the two basic tests.

## THE STEADY STATE LOAD TESTS

The steady state load test is accomplished by applying a steady force in one direction to a seal or bearing with 1.01" diameter and 0.75" length, and observing the resultant rotor displacement in both the direct axis (in direction of the applied load) and the quadrature axis (at right angles to the applied load). The steady load was incremented in 1/2-lb. steps at low eccentricity, and one pound steps at high eccentricity. Rotative speed was held constant for each run, using 100, 200, 300, and 400 rad/sec. Temperature of oil, incoming, at bearing, and outlet were controlled as carefully as possible, so that the lubricant in the bearing was at 70°F and 80°F, yielding dynamic viscosities for the T-10 oil used of 62.5 and 50 centipoise, respectively. Since the bearing studied in this test was a hydrostatic bearing, the oil pressure was also controlled, using 4 psi, 8 psi, 12 psi, and 15 psi. A family of dynamic stiffnesses was done for bearing diametrical clearances of 10 mils, 8 mils, and 5.5 mils.

A typical plot of the steady state direct and quadrature eccentricity for oil supply pressures of 4 and 15 psi as a function of load at 400 rad/sec of a 5.5 mil diametral clearance bearing at 80°F is shown in Fig. 1.

Figure 2 shows the same parameters plotted for the bearing with 8 mils diametral clearance.

Figure 3 shows the journal eccentricity as a function of load for the bearing with 5.5 mil diametral clearance at 15 psi oil supply pressure, temperature 80°F, and at rotative speeds 100, 200, 300, and 400 radians/sec.

Figure 4 shows the journal Eccentricity plot for the bearing with 8 mils diametral clearance.

Since the stiffness characteristics as functions of the eccentricity ratio are desired, the stiffness plots are developed by dividing the input steady force vector by the resultant steady state displacement vector. The resultant dynamic stiffness vector is then converted to rectilinear form, as in the perturbation tests reported in the papers [1-5]. The stiffness in the direction of the input force is called the S.S. (Steady State) Direct Dynamic Stiffness, and the observed stiffness at 90 degrees to the input force is called the S.S. Quadrature Dynamic Stiffness. Since perturbation speed is zero, all dynamically generated stiffness terms are zero in this test, thus the prefix "S.S." (Steady State) on the Dynamic Stiffness terms.

Some typical graphs of the S.S. Quadrature Dynamic Stiffness divided by rotative speed, and the S.S. Direct Dynamic Stiffness as functions of various families of parameter-changes are shown in Figures 5 through 9.

There is one more feature to the Steady State Quadrature Dynamic Stiffness that was observed and is worthy of noting; however, it was not more detailedly studied. Figure 10 (a) shows a sharp drop in this stiffness at high eccentricity. This regularly occurs at the "corner" of the Steady State Direct Stiffness term, shown in Figure 10 (b) (as above), and at the "corner" of the plot of position vs. load shown in Figure 10 (c).

This sharp drop is repeated for both increasing and decreasing load with very little hysteresis. In the basic equation:

Input Force=(Direct Stiffness)(Direct Motion)-(Quad Stiffness)(Quad Motion)

the principal load is carried by the Quadrature at eccentricities from 0 out to some higher eccentricity value. There often occurs a limit of the load carrying value of

this term, dependent on operating parameters. When the input force goes above this level, the attitude angle drops sharply from the 90° region toward zero. When this occurs, of course, the Direct term balances against the input force. This interesting behavior of the Steady State Quadrature Stiffness term has not been further researched, as it will not affect the instability onset from low eccentricity positions. It is, of course, active in determining orbital limit cycle size of an instability, and it may affect onset of instability from high eccentricity ratios.

## THE SQUEEZE FILM TESTS

For each bearing configuration, a set of Squeeze Film Tests were run following the Steady State Load tests. The Squeeze Film test is accomplished at zero rotative speed, with the journal at steady state centered in the bearing, and perturbing the rotor system with steps of increasing perturbation force. The input force is circular in nature, and for zero rotative speed, there is no concept of forward or reverse. With rotative speed at zero, all dynamic stiffness terms carrying $\omega_R$ (rotative speed) drop out.

The Squeeze Film dynamic stiffness coefficients are again obtained by dividing the input perturbation force vector by the resultant dynamic motion vector at each perturbation speed. Since the input is a circular force, and the bearing is circular, the resultant dynamic motion is symmetric, the horizontal and vertical stiffnesses are identical, so that either axis can be used to derive the Squeeze Film Dynamic Stiffness terms.

As before, the dynamic stiffness vector is converted to rectangular form. The dynamic stiffness in the direction of the force is called the S.F. (Squeeze Film) Direct Dynamic Stiffness term and the dynamic stiffness at 90° to the input force is called the S.F. (Squeeze Film) Quadrature Dynamic Stiffness. Since the S.F. Quadrature Stiffness is comprised solely of the term $+j\omega_p D$, the $\omega_p$ term is divided out for final presentation to show D as a function of eccentricity for the particular set of conditions being run. ($\omega_p$ is the perturbation speed, D is bearing radial damping.)

It may be noted that in the steady state tests, the quadrature stiffness term was plotted as $K_{QUAD}/\omega_R$ with the units lb sec/in, while in the squeeze film test the quadrature term was plotted as $K_{QUAD}/\omega_p = D$ lb·sec/in.

It should be noted that these terms are directly related by the oil swirling ratio $\lambda$ (lambda) as $K_{QUAD}/\omega_R = \lambda D$, where $\omega_R$ is rotative speed. The graphs in Figures 6 and 7 differ from those in Figures 11 and 12 by the factor $\lambda$. By dividing the corresponding plots, the value $\lambda$ is obtained. It is consistently constant for all speeds, bearing clearances, temperatures, pressures, and eccentricity ratios and is equal to 0.48.

The total Quadrature Dynamic Stiffness term for stability and other rotor studies is the sum of the steady state quadrature term and the squeeze film quadrature term:

$$K_{QUAD} = \underbrace{j\omega_p D}_{\text{(from SQZ Film)}} - \underbrace{j\lambda\omega_R D}_{\text{(from Steady State)}}$$

Figures 11 and 12 show the typical and summary results of the Squeeze Film test for damping as a function of eccentricity ratio. It may be observed that the damping term is quite independent of supply oil pressure and of perturbation speed.

The bearing radial damping coefficient D has been described for nearly 80 years as having the relationship to eccentricity of $D = \frac{D_0}{(1-e^2)^{3/2}}$ , where $D_0$ is damping coefficient at low eccentricity (sometimes an additional term of $(2+e^2)$ appears in the denominator, also).

The laboratory tests consistently show a much simpler relationship, mainly $D = \frac{D_0}{(1-e^2)^1}$ . The latter may be very simply derived by assuming motion in one axis in a squeeze film bearing, as Figure 13 shows.

$$D = \frac{D_0 C}{2h_1} + \frac{D_0 C}{2h_2} \qquad e = \frac{Z}{C} , \qquad h_1 = C-Z , \; h_2 = C+Z$$

$$D = \frac{D_0 C}{2}\left(\frac{1}{C-Z} + \frac{1}{C+Z}\right) = \frac{D_0 C^2}{(C^2-Z^2)} = \frac{D_0}{C^2(1-e^2)^1}$$

$h_1$ is thin film clearance due to motion.
$h_2$ is thick film clearance due to motion.
Z is radial displacement.
C is radial clearance.

The $D_0$ term is a function of dynamic viscosity $\eta$ where $\eta$ has units of $\left[\frac{\text{mass}}{(\text{length})(\text{time})}\right]$ or $\left[\frac{\text{lb sec}}{\text{in}^2}\right]$ so that D is expressed in $\frac{\text{lb sec}}{\text{in}}$ (English), or $\frac{\text{kg}}{\text{sec}}$ (metric). $D_0$ is also a function of cube of the bearing length.

Even though this derivation arises from a squeeze film (zero rotation speed) and one degree of freedom, it appears to work perfectly well for the general case. The value of $D_0$ has not been evaluated, and the variation of damping D with cube of bearing length was accepted without further checking.

Figure 14 shows the damping as a function of inverse cube of diametral bearing clearance for 5.5, 8, and 10 mils diametral clearance. It was pleasing to note that this term fairly closely follows the generally accepted rule.

Another interesting feature of the old standard derivation of the bearing coefficients is that it shows an interlocking relationship between the direct and quadrature terms. This series of studies, as well as prior perturbation studies, show that the direct and quadrature stiffness terms are virtually independent, except that direct damping and quadrature ("cross") spring are intimately related, with both containing D.

The Squeeze Film Direct Dynamic Stiffness term is by far the most complex of all the terms revealed by these two simple tests.

It contains at least the following individual terms:

(1) Any spring in parallel with the tested bearing.
(2) The rotor mass.
(3) The fluidic inertia effect.
(4) The hydrostatic spring.
(5) The highly nonlinear spring as a function of eccentricity and other parameters.

(Of course, when the rotor is also turning, there are even more terms in Direct Dynamic Stiffness.)

For this reason, the S.F. Direct Dynamic Stiffness for a given set of parameters is plotted versus the square of the perturbation speed. Typical graphs are shown in Figures 15 and 16.

The first feature is the extrapolation of this curve to zero speed, which yields the Direct (Static) Spring of the system. As may be observed, the obtained spring coefficient is the same as the coefficient yielded by a corresponding test at steady state loading. This spring is a linear function of oil supply pressure of the hydrostatic bearing.

The second feature is the negative slope of the plot. As in prior studies on perturbation, using minimum rotor system mass, this slope consists principally of the fluidic inertia effect. Since the effective rotor mass is identified to be $0.002 \frac{lb\ sec^2}{in}$, anything more than this is the fluidic inertia.

It may be observed that the fluidic inertia term exhibits dependence on viscosity, as its value is observably lower at 80°F than at 70°F. In prior studies [2-4], we showed the fluidic inertia term to have viscosity $\eta$ to zero power. This set of experiments shows viscosity $\eta$ dependence to first power. Further studies will be required to adjust this function, but meanwhile, a power of one change is not too bad.

Shown in Figure 17 is a typical group of plots of direct, static stiffness, which is yielded as a remainder of the S.F. Direct Stiffness with the rotor mass and fluid inertia term subtracted and plotted against eccentricity ratio. The graphs indicate nonlinearity of the direct stiffness variable with perturbation unbalance mass. The extreme complexity of the Direct Stiffness is easily observed from Figure 17 plots which cover a wide band of perturbation speed and input perturbation force levels.

## TESTS FOR THE VALIDITY OF THE MEASURED STIFFNESS TERMS

In order to check the validity of the dynamic stiffness terms obtained from the steady state load tests and the squeeze film tests, the same rotor/bearing system was then run under the similar conditions at the rotative speeds 2000 and 2500 rpm. At these speeds, forward and reverse perturbation loading was applied. This loading was supplied by perturbation imbalance weights at 1.25 inch radius of 1.75, 3.5, 7, 14, 28, and 56 grams. Total centrifugal force was limited to 16 pounds by limiting perturbation speed for the higher imbalance weights.

Figure 18 shows a summary of the results at 2000 rpm rotative speed, with oil supply at 70°F and 4 psi. It presents a plot of Direct Dynamic Stiffness vs. Perturbation Speed for the various perturbation loads. This figure also shows the displacement amplitude in pp mils vs. forward perturbation speed.

Of major interest here is the hump in the Direct Dynamic Stiffness term that occurs at the oil whirl resonance speed of about 1000 rpm. This hump occurs as the displacement motion moves from the nearly linear region of the S.S. Direct Stiffness region at low eccentricity, onto and above the "knee" of that curve (see Fig. 10b). The hump begins with the 14 gram perturbation imbalance and gets progressively higher as a function of the increasing perturbing force.

The Quadrature Dynamic Stiffness plots are not shown. They remain a straight sloping line, as is usual, except for an "S" shaped curve around 1000 rpm for high eccentricities. This is an indication that the swirling ratio does not remain constant in this region, which is a fairly necessary phenomenon for the proper description of whip instability and is being studied further.

It may be noted that the regular parabola caused by the rotor mass and fluidic inertia is distorted as the perturbation load increases. This interesting effect will modify the algorithm of fluidic inertia previously proposed [2-5], and is also being further studied.

## CONCLUSIONS

(1) It is believed that the steady state load test combined with the squeeze film tests can be used to evaluate the dynamic stiffness characteristics of seals and bearings.

(2) Whereas many researchers appear to have very capable computer programs for the determination of stability of rotating machinery, it is considered highly important to have the dynamic stiffness characteristics correlated as closely as possible to the actual rotor/bearing situation in order to get the best stability prediction results.

With improved knowledge of the dynamic stiffness nonlinearities as functions of eccentricity, it becomes possible to not only obtain the inception of instability, and its frequency, it is also possible to predict the size of the stable orbiting when an instability occurs.

## REFERENCES


1. Bently, D.E., Muszynska, A.: Stability Evaluation of Rotor/Bearing System by Perturbation Tests, Rotordynamic Instability Problems in High Performance Turbomachinery, Proc. of a Workshop, Texas A&M University, College Station, TX, 1982.

2. Bently, D.E., Muszynska, A.: Oil Whirl Identification by Perturbation Test. Advances in Computer-aided Bearing Design, ASME/ASLE Lubrication Conference, Washington, DC, October 1982.

3. Bently, D.E., Muszynska, A.: Perturbation Tests of Bearing/Seal for Evaluation of Dynamic Coefficients. Symposium on Rotor Dynamical Instability, Summer Annual Conference of the ASME Applied Mechanics Division, Houston, TX, June 1983.

4. Bently, D.E., Muszynska, A.: The Dynamic Stiffness Characteristics of High Eccentricity Ratio Bearings and Seals by Perturbation Testing. Workshop on Rotordynamic Instability Problems in High Performance Turbomachinery, Texas A&M University, May 1984.

5. Bently, D.E., Muszynska, A.: Perturbation Study of Rotor/Bearing System: Identification of the Oil Whirl and Oil Whip Resonances. Tenth Biennial ASME Design Engineering Division Conference on Mechanical Vibration and Noise, Cincinnati, OH, September 1985.

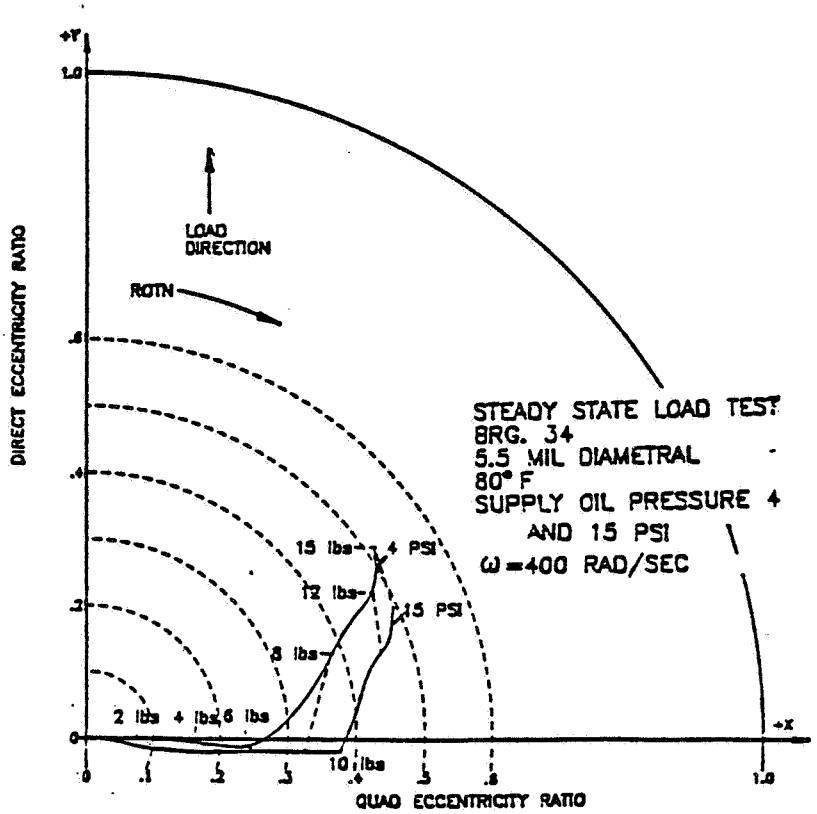


Figure 1.

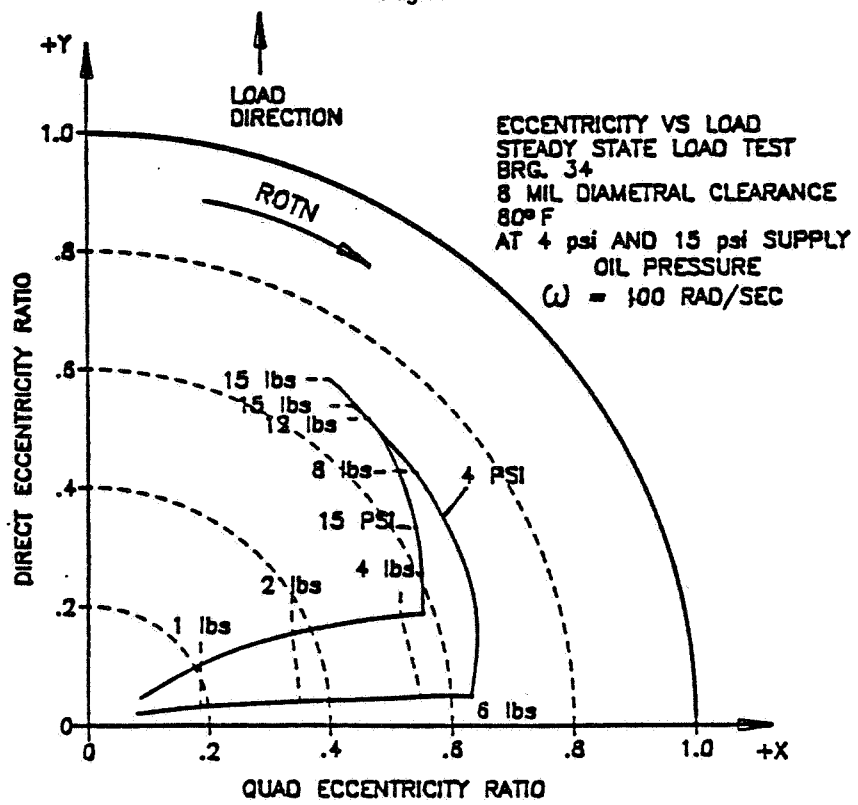


Figure 2.

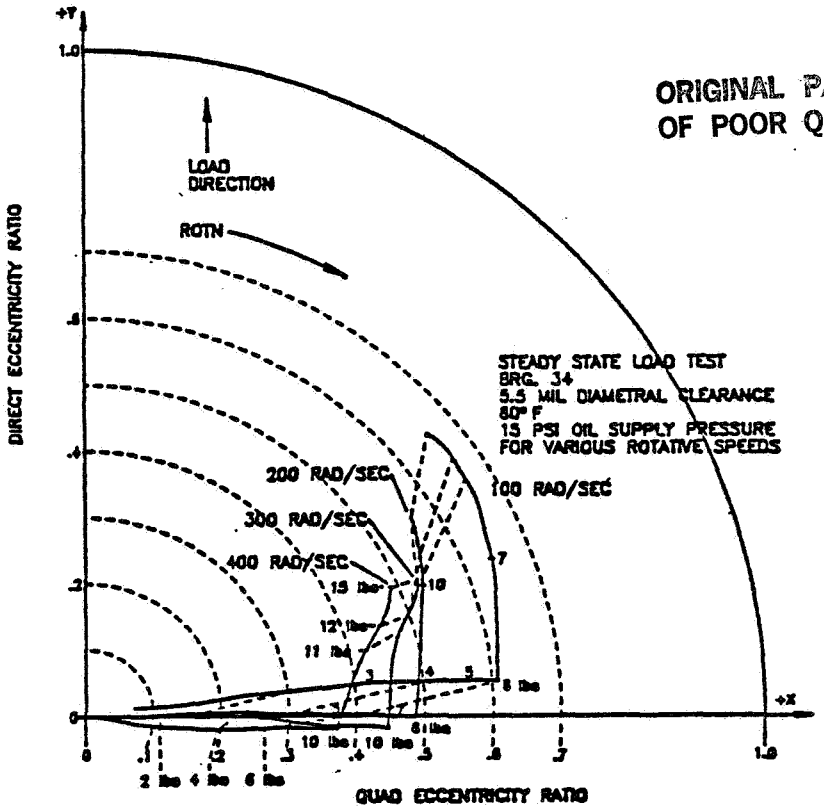


Figure 3.

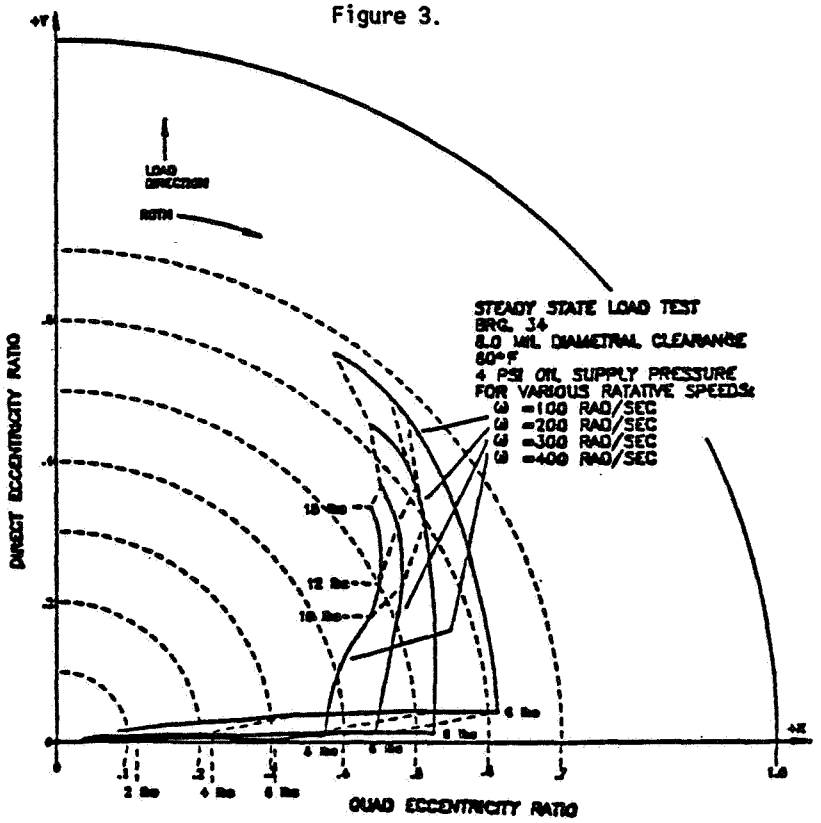


Figure 4.

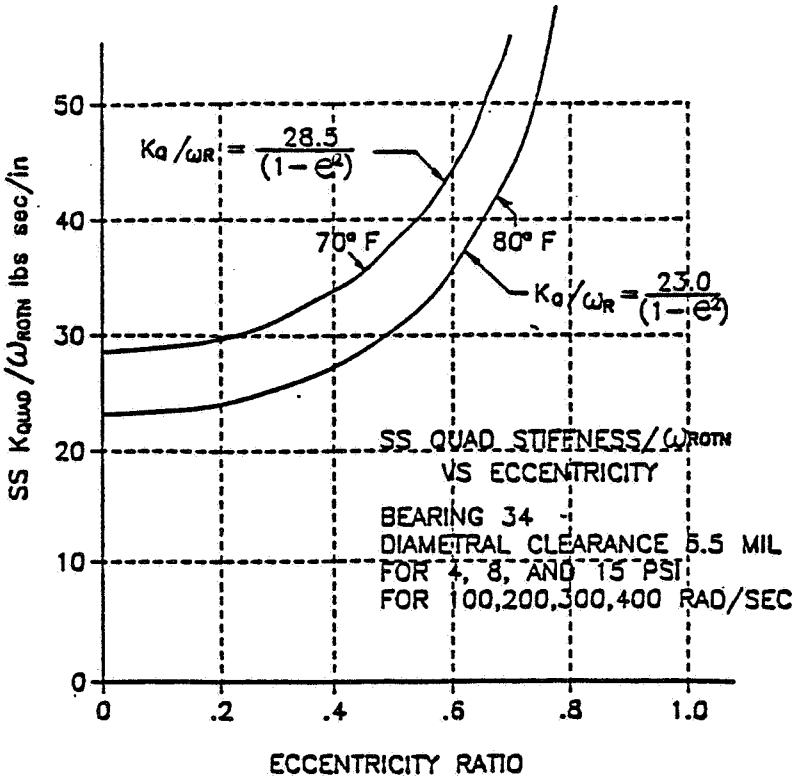


Figure 5.

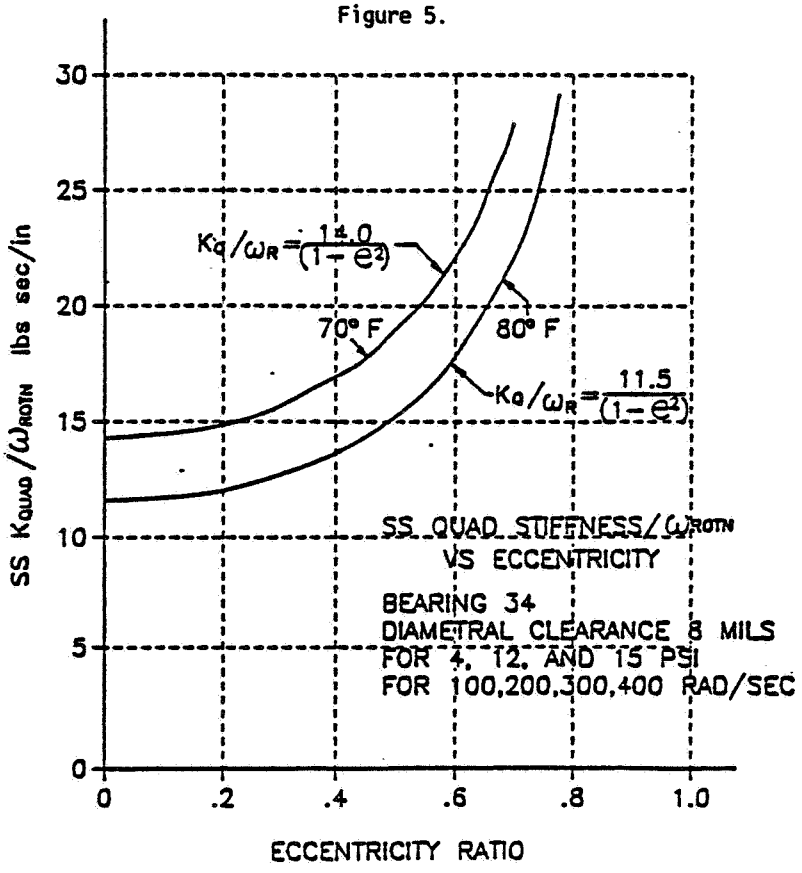


Figure 6.

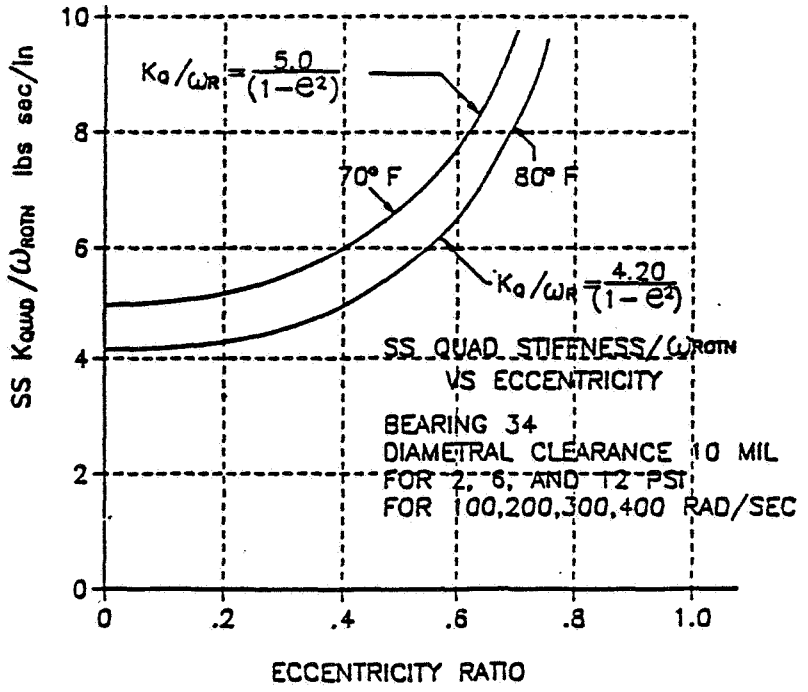


Figure 7.

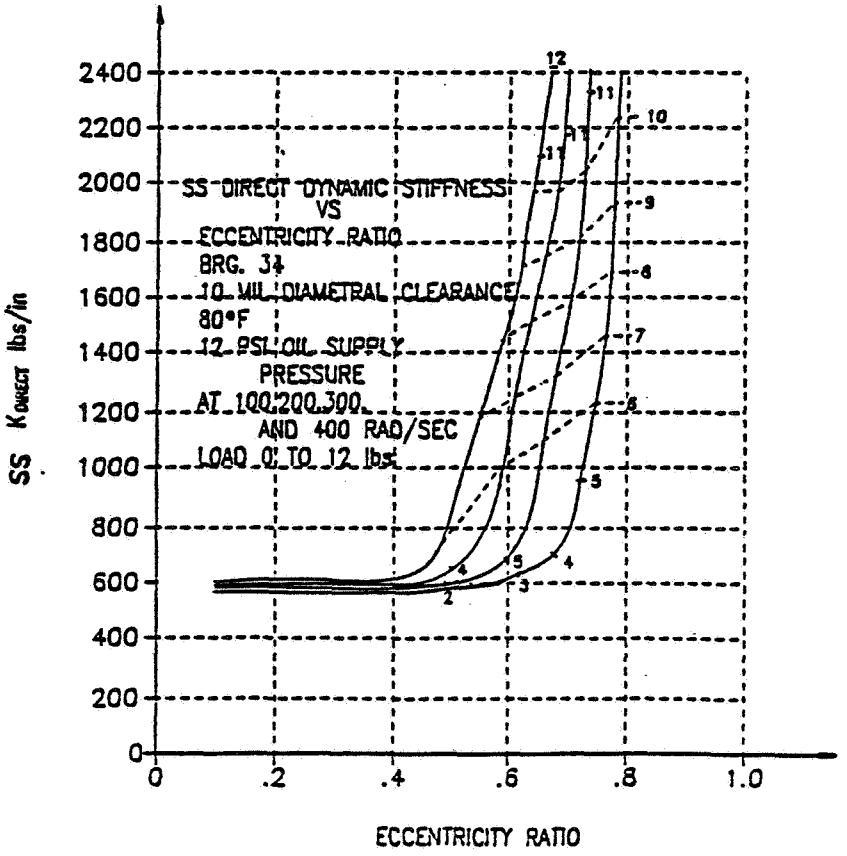


Figure 8.

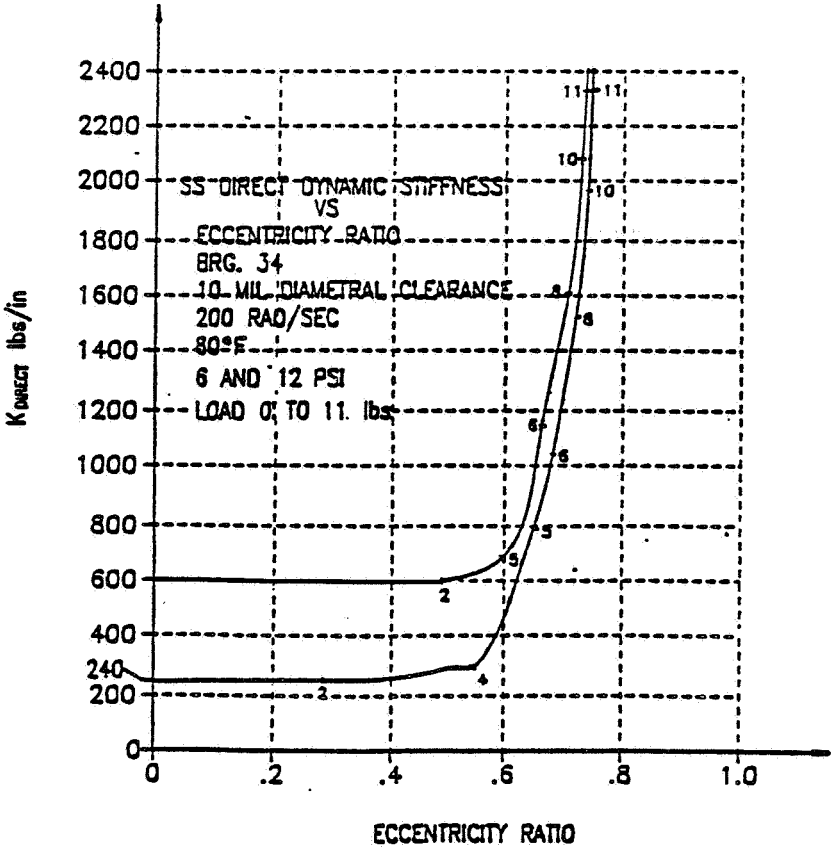


Figure 9.

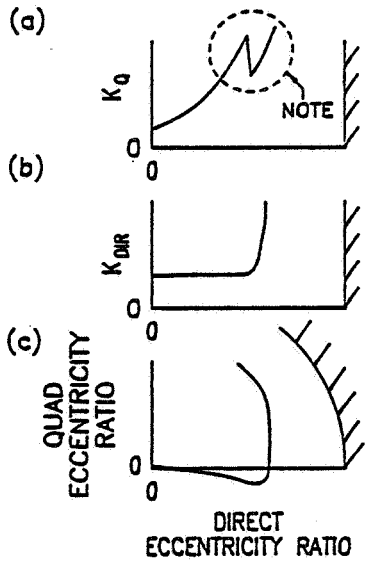


Figure 10.

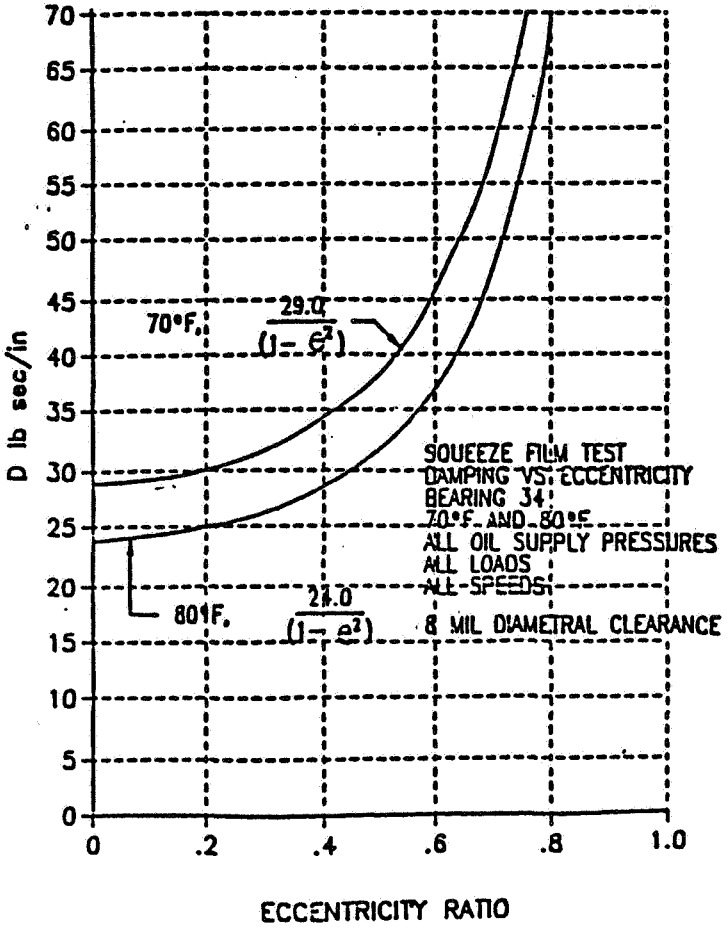


Figure 11.

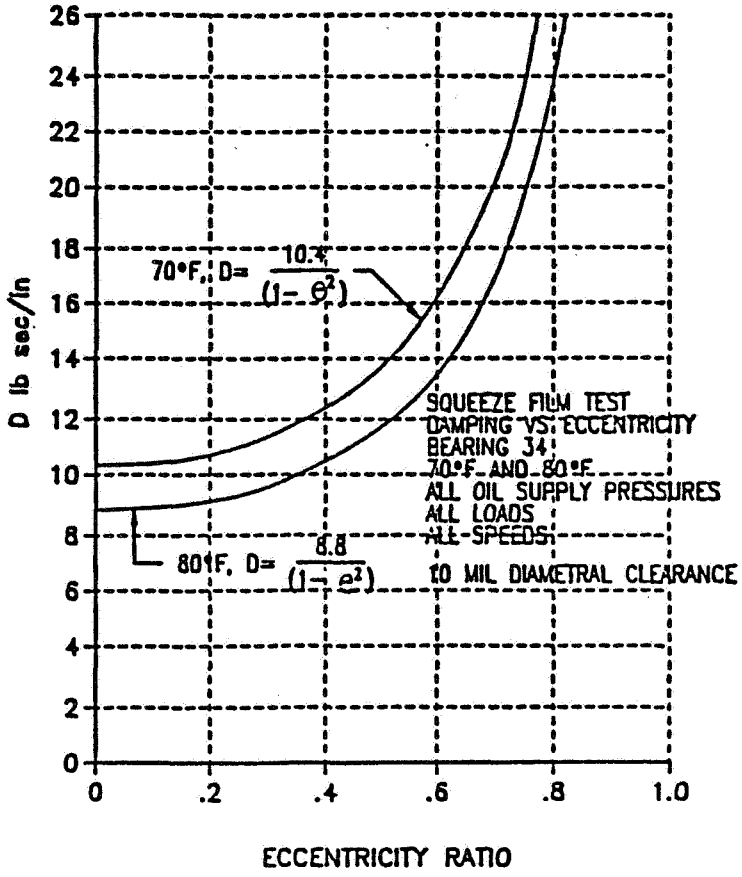


Figure 12.

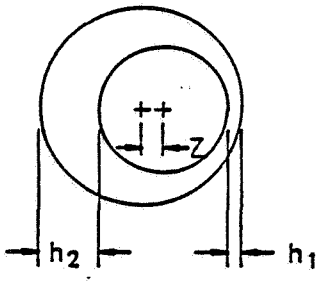


Figure 13.

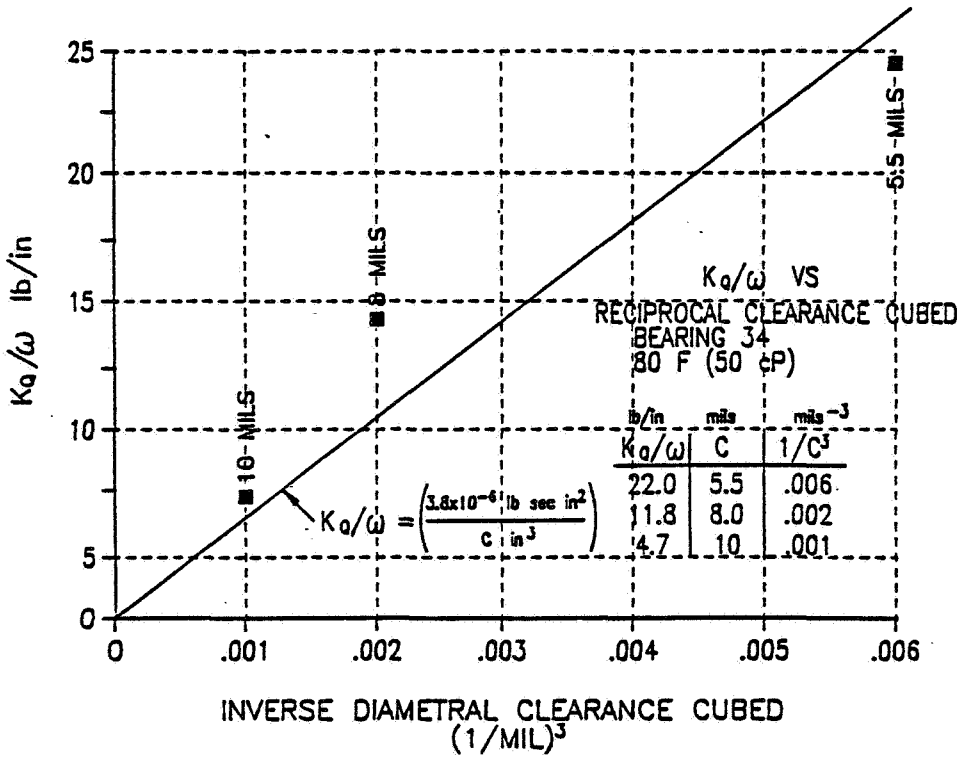


Figure 14.

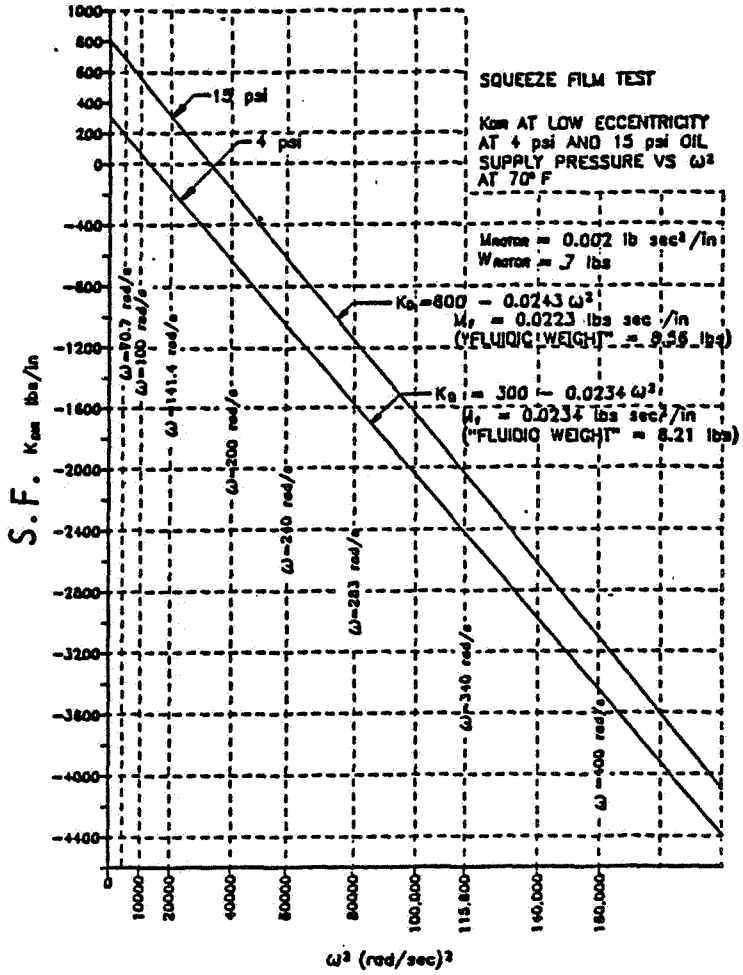


Figure 15.

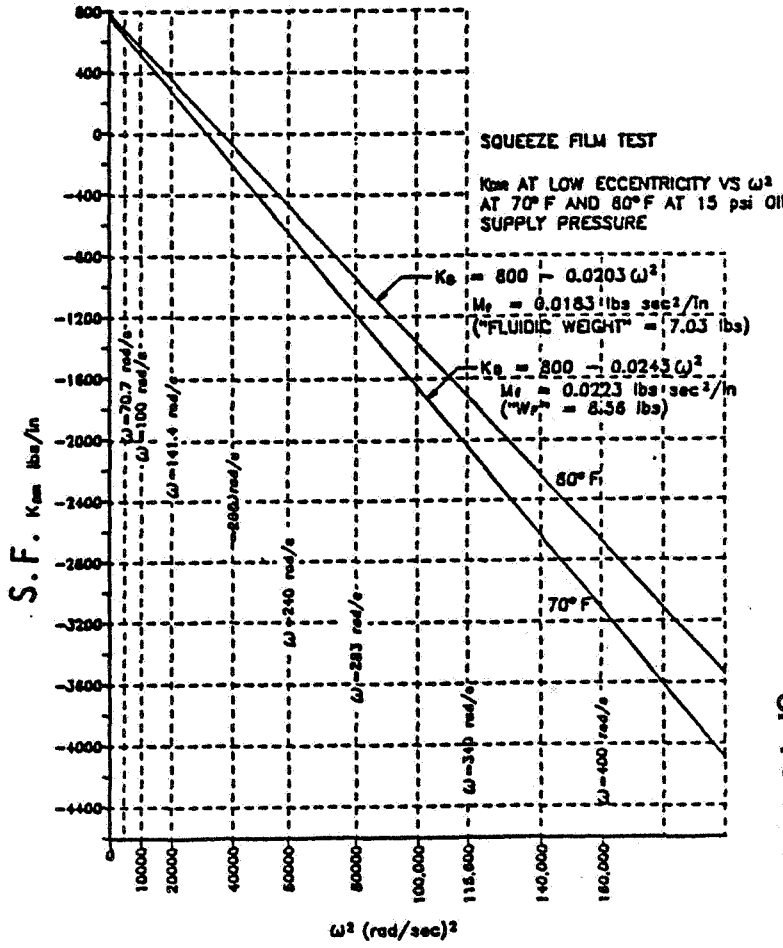


Figure 16.

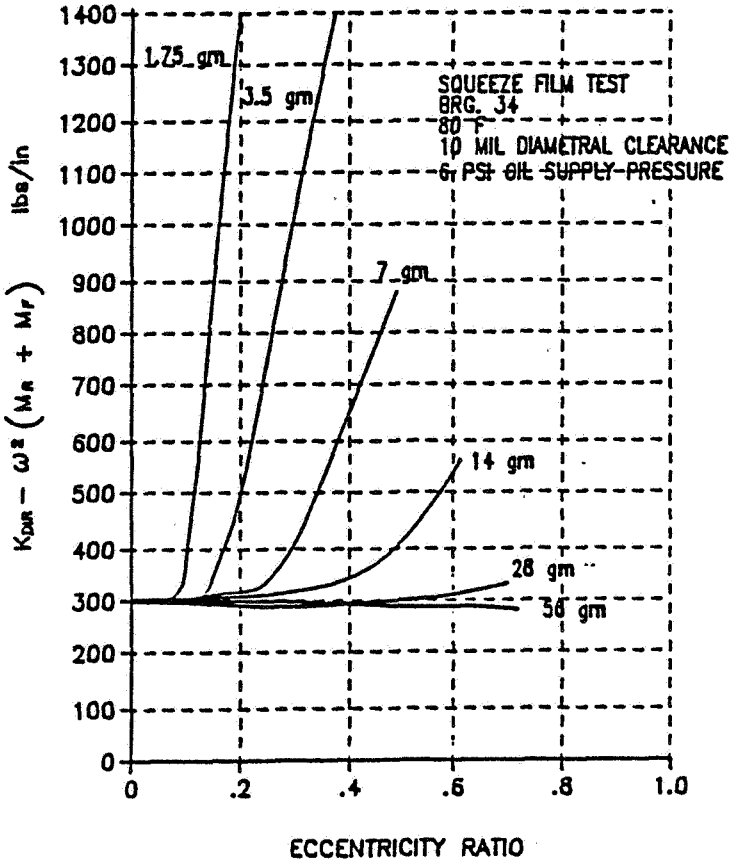


Figure 17.

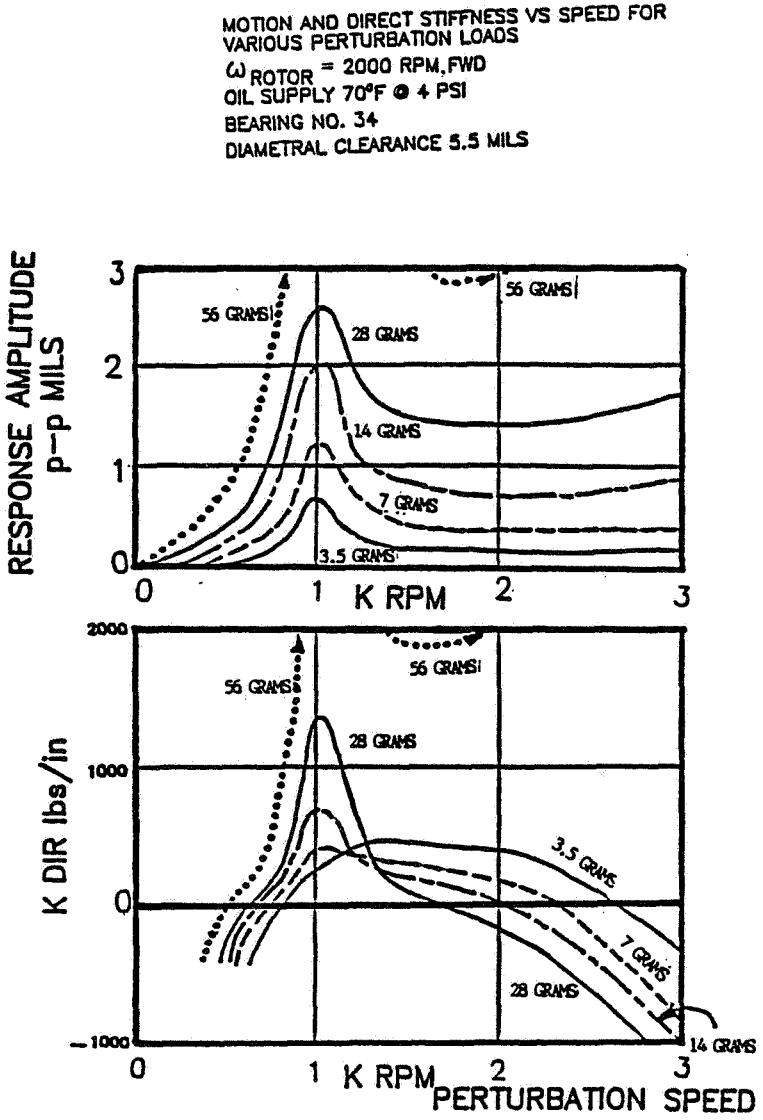


Figure 18.